Character of the insulating state in NiO: A mixture of charge-transfer and Mott-Hubbard character

T. M. Schuler,* D. L. Ederer, and S. Itza-Ortiz†
Department of Physics, Tulane University, New Orleans, Louisiana 70118, USA

G. T. Woods‡ and T. A. Callcott
Physics and Astronomy Department, University of Tennessee, Knoxville, Tennessee 37996, USA

J. C. Woicik
National Institute of Standards and Technology, Gaithersburg, Maryland 20899, USA
(Received 12 July 2004; published 18 March 2005)

Using site-specific soft x-ray emission and absorption spectroscopy in conjunction with site-specific x-ray photoelectron spectroscopy, we present measurements of the valence and conduction band states of NiO. Significant hybridization between the Ni and the O electronic states near the Fermi energy is observed throughout both the valence and conduction bands, in accordance with density-functional theory calculations also presented. The relationship between our emission and absorption measurements also shows direct similarities to other techniques used to measure the non-dipole-allowed *d*-*d* transitions within NiO, addressing questions concerning the character of the insulating band gap of this system. NiO has previously been described as a large-gap, charge-transfer insulator, while our data show the valence and conduction states at the Fermi energy to be primarily of Ni *d*–character hybridized with a small amount of O *p*–character states, suggesting a mixture of charge-transfer and Mott-Hubbard character as described by the Zaanen-Sawatzky-Allen model.

DOI: 10.1103/PhysRevB.71.115113 PACS number(s): 71.20.Be, 78.70.Dm, 78.70.En, 68.49.Uv

INTRODUCTION

The recent push for innovative magnetic materials has prompted a number of studies[1–4] on first-row transition-metal monoxides, due to their interesting electronic and magnetic properties. For many of the properties of these materials (including MnO, FeO, and CoO), NiO has historically been used as the model system to describe the aspects of their electronic structures,[5,6] although questions still arise as to theoretical characterizations of the electronic structure and bonding for NiO and related materials. NiO is a high-spin antiferromagnetic (AF) insulator with a Néel temperature (T_N) of 525 K.[7] Its crystal structure is that of rocksalt, which is cubic above T_N but becomes a contracted rhombohedral cell below T_N due to a slight distortion in the direction of the antiferromagnetic ordering of the adjacent ferromagnetic planes.[8] However, because local magnetic ordering persists above T_N, valence band photoemission spectra show no significant changes as the sample temperature is raised above T_N.[9] NiO has been shown to exhibit magnetostrictive behavior, which is due to the movement of the antiferromagnetic domains in which the spins are confined within the octahedral planes, although this behavior appears to have a minimal effect on the coupling of the electron orbitals.[10] The concentration of magnetostrictive behavior in the domain walls has been observed recently by using the absorption of linearly polarized synchrotron radiation absorption and spectromicroscopy at the Ni L_2 edge to map out AF domain boundaries.[11] Recent theoretical work has also shown NiO to exhibit subpicosecond switching characteristics,[12] illustrating the potential applications of this material in the field of spintronics.

Many of the problems with *ab initio* calculations on transition-metal oxides can be traced to the fact that their partially occupied metal *d* states seem incompatible with their insulating properties. The electronic structure of NiO is complicated by strong correlation effects arising from Coulomb repulsion in the partially filled shell, causing a splitting of the Ni 3*d* minority band into two Hubbard subbands—giving rise to a *d*-*d* insulating gap and thus making it appropriate to designate the compound a Mott-Hubbard insulator.[8] Further complexities are introduced by the level of hybridization (chemical bonding) between the Ni 3*d* and O *p* states in the valence and conduction bands. Experiments and theoretical calculations have suggested that the insulating character of NiO arises from a charge-transfer mechanism with both localized and delocalized states;[13] however, band structure calculations based on this model generally report a band gap of $\sim$0.2 eV,[14] which is much smaller than that usually found experimentally ($\sim$4 eV).[15–17] Although this discrepancy has been shown to arise from derivative discontinuities of the exchange-correlation energy within density-functional theory (DFT) which occur when working with insulating systems,[18] attempts to adjust calculations to reconcile with experimental results have yet to present a definitive solution.[14,19]

One issue at the heart of this matter is the inability of most modern spectroscopic techniques to directly measure the so-called "*d*-*d* gap" between the Hubbard-split minority 3*d* states in Ni, owing to the restrictions of the dipole approximation ($\Delta\ell = \pm 1$). Measuring dipole-allowed transitions across the Fermi energy would describe the optical gap between valence and conduction states; however, it does not necessarily measure the true insulating band gap, defined as

the energy difference between occupied and unoccupied electronic states. Several techniques have recently been developed with the intent of measuring transitions across the insulating band gap by circumventing the dipole restrictions or performing measurements at low energies where dipole restrictions are relaxed. While soft x-ray emission spectroscopy is subject to the dipole selection rules, the use of conjunctional techniques such as resonant inelastic x-ray scattering near the absorption threshold allow direct measurements of the *d*-*d* gap in strongly correlated materials[2,20] comparable to excitations measured by low-energy techniques such as second-harmonic generation[21,22] (SHG) and spin-polarized electron energy-loss spectroscopy (SPEELS).[23,24]

Using several different spectroscopic techniques we have measured the electronic valence states at the Fermi energy (E_F) of NiO in order to develop a more complete picture of the Ni $3d-$O $2p$ hybridization within this region and further discuss issues concerning the measurement and characterization of optical and insulating band gaps. Soft x-ray emission and absorption spectroscopy (XES and XAS, respectively) provide the ability to measure excitations across the Fermi edge and probe element- and site-specific states in both the valence and conduction bands of NiO. XAS, or more specifically near-edge x-ray absorption fine structure (NEXAFS) spectroscopy, involves the photon excitation of a core-level electron into the conduction band of the material, mapping the absorbing states above E_F. XES is a first-order process occurring when an electron from a higher-energy state fills a core hole left by the photoexcitation of a core-level electron, releasing a photon in the process. By measuring the energy of the emitted photons, one can map the excited state properties of the system's valence band. Figure 1 contains two diagrams describing resonant (a) and nonresonant (b) x-ray measurements of NiO. The ground state (GS) of NiO is mixed, consisting of a linear combination of the normal ground state (Vd^8) and a charge-transfer state ($Vd^9\underline{L}$). There is also understood to be a small admixture of $Vd^{10}\underline{L}^2$ states that will not be discussed in this description. The quantity V denotes the valence band and $\underline{L}$ represents a ligand hole. The valence band (V) shown in Fig. 1 is composed of mostly O $2p$ states and hybridized Ni $3d$ states, with the more localized $3d$ band being depicted by the shaded narrow rectangles, lying at slightly higher energies than the O $2p$ band, shown as hollow rectangles. Resonant excitation [Fig. 1(a)] involves the absorption of an x-ray producing a core hole ($\underline{c}$) and an electron in the conduction band, yielding a NEXAFS describing the conduction states as presented in this paper. These states may relax via elastic or inelastic scattering in resonant x-ray emission spectroscopy (RXES) or Auger emission (not shown), producing a spectrum whose final state may result in the transfer of an electron to an excited state having the same parity as the ground state (*d*-*d* excitations). Resonant x-ray emission measurements have recently been reported[25] describing charge-transfer and *d*-*d* transfer processes in NiO.

The emission measurements presented in this study are concerned with the nonresonant excitation of electrons in NiO, a process depicted in Fig. 1(b). In this situation, the initial state for the x-ray process is the removal of a core

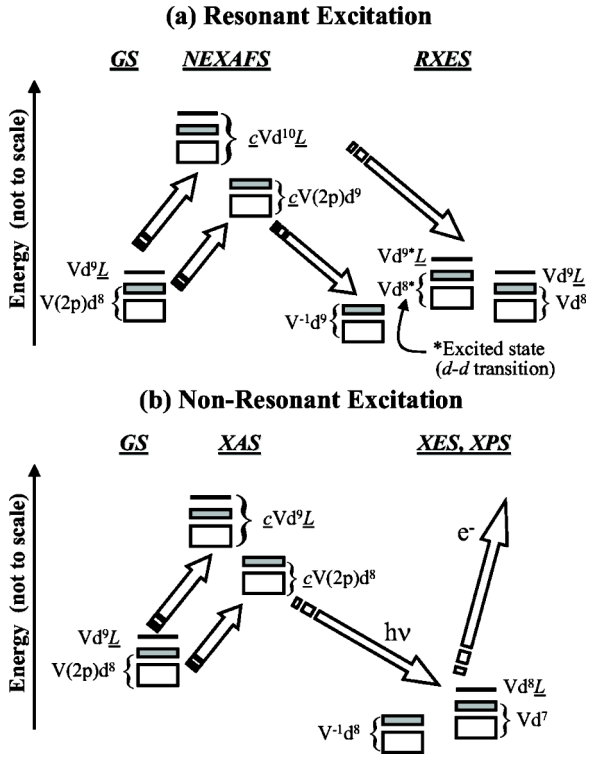

FIG. 1. Electronic diagrams describing ground and final states for resonant (a) and nonresonant (b) excitation measurement processes in NiO. In this diagram, V indicates valence band electrons, the arrows represent photon absorption or emission, and $\underline{c}$ and $\underline{c}$ denote core and ligand holes, respectively.

electron by x-ray absorption, allowing the excited state to relax part of the time by x-ray emission to the final states shown at the far right of Fig. 1(b). The site specificity of the XAS and XES processes is advantageous over standard photoemission measurements, which give generalized valence band information without regard to the atom or site. We also present a comparison of XES spectra with measurements of NiO using site-specific x-ray photoelectron spectroscopy (SSXPS),[26] a technique that can directly obtain individual atom-enhanced valence band information by generating a standing wave of incident and reflected x-ray beams near an x-ray Bragg reflection and placing the maxima of the electric-field intensity on the desired atom within the unit cell to measure the x-ray photoelectron spectra from that site.[27] The x-ray photoelectron spectroscopy process occurs with a photon being absorbed by a valence band electron in the ground state, resulting in the ejection of the electron from the material, giving a final state identical to that which is produced by XES, as displayed in Fig. 1(b).

By comparing the above described experimental techniques with density-functional theory electronic structure calculations, we find that NiO has characteristics of both a charge-transfer insulator and a Mott-Hubbard insulator owing to the high level of hybridization between Ni $3d$ and O p states both above and below E_F. The magnitude of the insulating and optical gaps from our measurements is shown to be comparable to that measured by other techniques.

EXPERIMENT AND CALCULATIONS

All measurements presented here were performed on a NiO single-crystal sample; measurements performed on powdered NiO samples showed no difference from the single-crystal measurements. The XES and XAS measurements were made at beamline 8.0.1 of the Advanced Light Source located at Lawrence Berkeley Laboratory, which is an undulator beamline equipped with a spherical grating monochromator as described by Jia *et al.*[28] The experimental configuration consisted of linearly polarized, monochromatic soft x rays directed onto a sample to generate core-electron excitations. Photons that have fluoresced from the sample pass into the spectrometer chamber, where a spherical grating diffracts them to a multichannel detector positioned along the Rowland circle to obtain the desired energy range. The angle of incidence for the sample was set to 45° in order to maximize detection of the emitting photons; measurements performed at other sample angles exhibited no discernable spectral variation.[29] The incident and emitted photon energies were calibrated to within 0.5 eV accuracy using previously published[30–32] energy values. The SSXPS measurements were performed on beamline X24a of the National Synchrotron Light Source. The Ni(001) crystal was aligned so that the (111) diffracting planes were normal to the synchrotron beam and the electron-emission spectra were recorded with a multichannel hemispherical analyzer. Photoelectron spectra were collected at different photon energies around the Bragg condition by setting the photon energy and scanning the electron analyzer in a high-resolution mode. In these measurements, the electron energy resolution was ~0.35 eV and the photon energy width was ~0.45 eV. Details of the SSXPS experimental process have been published elsewhere.[26]

The Ni 3*d* and O 2*p* density of states (DOS) were calculated by means of the WIEN97 code[33] employing the full-potential linear augmented plane-wave method within DFT. The exchange-correlation term was treated using the generalized gradient approximation (GGA),[34] which deals with radial and angular gradient corrections, and has been shown to be superior to the corresponding local-density approximation (LDA) in determining the structural properties of transition metals.[35] Our GGA calculation was performed without the use of a Hubbard U parameter[36] which is used in conjunction with the LDA to account for the strong *d*-*d* Coulomb interactions that split the Ni 3*d* band and open the insulating gap wider than standard DFT models usually predict. With the exception of predicting a smaller band gap, our DOS closely resembles LDA calculations using a Hubbard parameter $U=5$ eV, while similar calculations with $U=8$ eV display a very different gap width and insulating character than our calculations.[37]

RESULTS

Figure 2 shows our calculated DOS of NiO describing states near the Fermi edge. In this figure, the Ni 3*d* DOS is split into the spin-polarized majority (↑) and minority (↓) spin states, while the O *p* states are not spin resolved. The calculation produces an antiferromagnetic ground state with a band gap of about 1.2 eV, having the largest density of states above and below the Fermi energy ($E_F=0$ eV) belonging to the Ni 3*d* band. The greatest weight of O *p* states in the valence band is located at −5 eV, and in the conduction band at 1.5 eV. The diminished spectral weight of the O *p* states near E_F suggests that the insulating gap is characterized mainly by *d*-*d* excitations in the Ni atoms, implying a gap of Mott-Hubbard type. However, a large level of *p*-*d* hybridization between the O and Ni ions is evident throughout the DOS plot, with nearly complete hybridization at the main O site (−5 eV), and the O states making small contributions just below and above the Fermi edge. The O 2*p* states are hybridized mainly with Ni 3*d* majority spin states at energies well below E_F, and with minority spin states at and above E_F. Though the weight of these hybridized O states is small near the Fermi edge, they could imply an insulating gap containing a level of charge-transfer character.

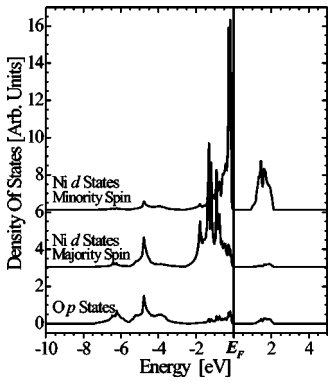

FIG. 2. DFT-calculated partial densities of states for O *p* states and spin-polarized Ni *d* states near the Fermi energy (0 eV). Hybridization between the O and Ni states is seen throughout the spectra, and initial peaks below and above E_F are Ni 3*d* minority spin states.

In Fig. 3 we show a comparison of the calculated DOS (a) from Fig. 2 with a convolution of the DOS (b), and XES measurements of NiO describing valence states near the Fermi edge (c). In plot (a) the Ni 3*d* DOS (shaded gray) is displayed as the sum of the majority and minority spin states for comparison with the XES measurements, which are insensitive to spin polarization. In order to compare our calculated partial DOS (PDOS) to XES measurements of the valence band, Fig. 3(b) shows the result of a convolution of the DOS from Fig. 3(a) with a Gaussian function of width (full width at half maximum 1.50 eV for O states, 2.75 eV for Ni states) comparable to the resolution of our emission measurements ($E/\Delta E=300$). In the convolved PDOS plots we see a small O peak just below the Fermi energy which is aligned with the main peak of the convolved Ni PDOS, indicating a significant contribution of the O states resulting from their hybridization with the Ni 3*d* states at the top of the valence band, particularly the Ni 3*d* minority spin states which have the largest presence at that energy. A similar effect is seen at the main peak of the convolved O 2*p* PDOS, where a low-energy shoulder in the Ni 3*d* spectrum is aligned with the main peak of the O 2*p* spectra, indicating significant hybridization between Ni and O electronic states at higher binding energies as well.

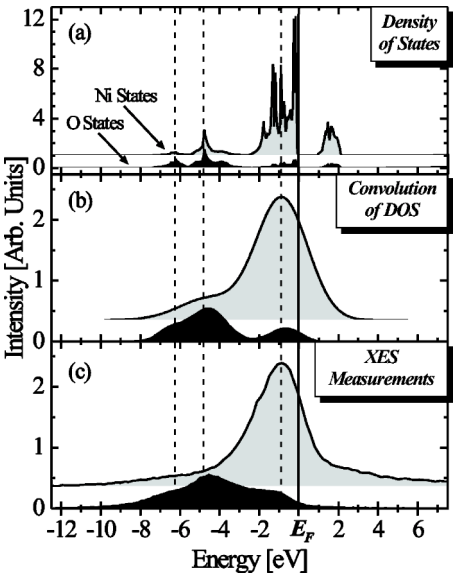

FIG. 3. Calculated PDOS (a) for Ni (top spectra, shaded gray) and O (bottom spectra, shaded black) sites and the convolution (b) of the DOS to resemble spectral resolution, compared with experimental XES measurements (c). The transitions displayed in plot (c) are $\underline{c}(2p)Vd^8 \rightarrow Vd^7$ (Ni spectra) and $\underline{c}(1s)Vp^4 \rightarrow Vp^3$ (O spectra) in regard to Fig. 1(b).

Comparable features are seen in our site-specific XES results in Fig. 3(c), with measurements of the Ni L_3 emission (shaded gray) and the O K emission (shaded black). The XES measurements displayed in Fig. 3(c) are the result of valence band electrons filling core holes in Ni or O ($2p^5 3d^8 \rightarrow 2p^6 3d^7$ or $1s^1 2p^6 \rightarrow 1s^2 2p^5$, respectively) resulting in an excited final state consisting of a valence hole. The excitation energy producing the core hole was set well above the binding energy required in order to eliminate resonant processes, and the measured spectra have been scaled to match the relative intensities of the convolved DOS, which are also in accordance with theoretical atomic cross sections.[38] The Ni spectra shows one major peak located about 1 eV below E_F representing emission from 3d valence sites, which overlaps the Fermi energy due to the limited resolution of the spectrometer. The O emission plot shows deexcitation from the 2p valence levels, with one main peak located approximately 4 eV below E_F and a lower-intensity shoulder aligned with the aforementioned Ni 3d peak, showing the hybridization between the states just below the Fermi edge. The peak structures and energy positions in plots (b) and (c) are in good agreement, leading us to conclude that our DFT GGA calculation provides a suitable model for measurement comparison. Our placement of the valence band maximum (E_F) according to the calculated DOS is in accordance with arguments provided by Hüfner *et al.*,[39] who stated that it should be placed immediately above the highest valence band states, whereas experimental resolution factors may cause measurements to overlap the Fermi edge as shown in our spectra.

The ability to determine the valence band maximum of our measurements allows comparison to other experimental measurement techniques, such as photoemission spectra and

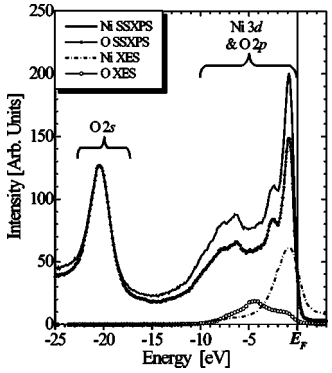

FIG. 4. A comparison of valence state measurements using XES and SSXPS experimental techniques. The spectra show comparable peak structure just below the valence band maximum (0 eV), and the Ni and O SSXPS spectra show nearly complete hybridization.

EELS spectra. Figure 4 shows the XES measurements previously displayed in Fig. 3(c) compared with site-specific x-ray photoemission spectroscopy measurements also performed on NiO.[26] Unlike XES, XPS samples states of all angular momenta and can allow a higher-resolution spectral picture of the valence band. The spectra presented in Fig. 4 display the valence band of ionic NiO recorded near the NiO (111) Bragg back-reflection condition with the electric-field intensity maximum positioned to give atom-enhanced photoelectron spectra of the Ni and O valence electrons. The spectra have been normalized to the height of the peak denoting the O 2s states (−21 eV) for comparison at E_F. The spectra show strong resemblance to the XES measurements, with the Ni 3d peak located ~1 eV below E_F, and peaks at lower kinetic energy representing the O 2p states. These spectra also suggest that the contribution of the O 2p states to the valence band is very small compared to that of the Ni 3d states, similar to the contribution level produced by our calculated DOS as well as the theoretical atomic cross sections.[38]

The level of hybridization between oxygen and nickel states below E_F is obvious from our measurements, and the specific peak overlap between O and Ni measurements can be seen at several points throughout Figs. 3 and 4. From the XES plots we see a high-energy shoulder associated with the O K emission peak located at nearly the same energy position as the Ni L_3 emission peak (−1 eV), indicating O 2p states mixing with the Ni 3d states near E_F. The L_3 peak of the Ni spectrum also presents a slight low-energy peak aligned with the main peak of the O spectrum (−4.5 eV) as well as a general asymmetrical broadening of the low-energy side of the peak maximum, all of which are suggestive of the influence of O p valence electron states on the Ni 3d states. The hybridization between the electron states below E_F is evident in the site-enhanced spectra, where the general spectral structure is nearly identical regardless of the elemental atoms being targeted. The only significant variation between the two spectra is the intensity of the peak structure between −15 and 0 eV (E_F) representing the Ni 3d and O 2p states, indicating an almost complete hybridization between Ni and O states above the O 2s electron level. The SSXPS spectra portray a situation very similar to that which is shown in the calculated DOS spectra, where the O 2p states which make

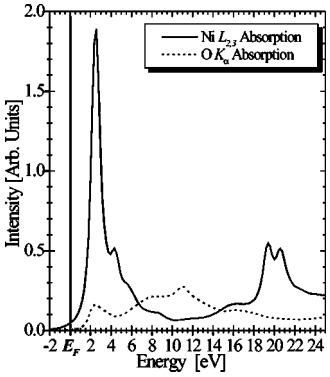

FIG. 5. X-ray absorption (NEXAFS) spectra measuring the conduction states of *d* character (Ni $L_{2,3}$) and *p* character (O *K*) above E_F (0 eV). Hybridization between *p* and *d* states is seen throughout the spectra, most notably at the initial peak (2.5 eV) indicating a mixture of *d*-*d* and charge-transfer insulating character. The transitions displayed in this figure are $Vd^8 \rightarrow c(2p)Vd^9$ (Ni spectra) and $Vp^4 \rightarrow c(1s)Vp^5$ (O spectra) in regard to Fig. 1(a).

up only a small proportion of the valence band states are completely hybridized with the larger number of Ni 3*d* states.

X-ray absorption measurements shown in Fig. 5 suggest that this hybridization is not limited to the valence band of NiO, and some hybridization is present in the core-hole excited states above E_F. The XAS (NEXAFS) measurements displayed in this figure are total electron yield absorption spectra for the Ni $L_{2,3}$ edge and the O *K* edge of our NiO single-crystal sample. The energy positions of these spectra have been scaled according to their respective valence band maxima, which were determined from a comparison between our XES measurements and the convolution of the corresponding DOS spectra. The zero-energy point in this plot (indicating the Fermi energy) is set at the same absolute energy as in the XES measurements displayed in Fig. 3(c). The intensity of the spectra has also been scaled to reflect the respective absorption coefficients of the elements involved.[38]

The structure of the Ni spectra is determined by the dipole-allowed transition from the subset of ground states ($2p^6 3d^8$, $2p^6 3d^9 \underline{L}$, and $2p^6 3d^{10} \underline{L}^2$, where $\underline{L}$ denotes a ligand hole) to a subset of final states consisting of ($2p^5 3d^9$) structure and related states ($2p^5 3d^{10} \underline{L}$ and $2p^5 3d^{10} \underline{L}^2 4s$), which are subject atomic spin-orbit, Coulomb exchange, and crystal-field interactions. Of primary concern are the peaks near the L_3 absorption edge of Ni, which correspond to the absorption of $2p_{3/2}$ spin-orbit-coupled core electrons and represents the bottom of the Ni conduction band in the presence of a 2*p* hole in our measurement. The major Ni L_3 peak located ~2.5 eV above E_F and its subsequent minor peak (~4.3 eV) can be attributed to the lowest-energy multiplets of the final state configuration ($2p^5 3d^9$) which includes a crystal-field splitting term ($10Dq$) of about 2 eV. The appearance of additional peaks above the main L_3 absorption peak is produced by the presence of the charge-transfer state[40] ($3d^9 \underline{L}$) and additional terms of the $2p^5 3d^9$ configuration modified by the crystal field.[41] The initial peak of the O *K*-edge absorption spectra can be attributed to the hybridized O 2*p* weight in states of the transition-metal 3*d* band, as observed by its alignment with the Ni 3*d* spectra approximately 2.5 eV above E_F. The spectral structure beginning 5 eV above the absorption threshold and extending as far as 20 eV into the conduction band and continuum states represents the hybridization of the O *p* states with the Ni 4*s* and 4*p* states.[31] The comparison of these measurements resembles EELS measurements performed at the Ni *K* edge, Ni $L_{2,3}$ edge, and O *K* edge by Grunes,[42] which show states of *p* character (from *K*-edge measurements) aligned with the initial peak of the Ni $L_{2,3}$ EELS spectra, which is a measure of *d*-character states.

Throughout these spectra we see several points suggestive of hybridization between the Ni and O electronic conduction states. From the obvious overlap of the initial peaks at 2.5 eV to the small feature at ~17 eV, nearly every feature in the O *K* absorption spectrum shows a corresponding feature in the Ni $L_{2,3}$ absorption spectrum. Obviously, the most significant of these is the overlap of the initial peaks in each spectrum, indicating a substantial mixing of *d*-character and *p*-character states immediately above the Fermi edge. As shown by our DOS calculations, the number of O *p* states is considered small compared to the number of Ni 3*d* states; however, this hybridization again raises questions concerning the characterization of the states making up the top and bottom of the insulating gap in NiO. There are several points at which hybridization appears to be noticeably lacking, specifically the second and third peaks of the Ni spectra (4.3 and 5.8 eV, respectively), which are attributed to excited state multiplets of Ni states, and the largest peak of the O spectra (11.0 eV), attributed to hybridization of O *p* states with Ni 4*s* and 4*p* states, which are not detected by dipole-restricted XAS measurements in the Ni spectrum, as has been previously suggested.[40]

The hybridization of valence states at E_F has direct impact on the problem of characterizing the insulating gap as being of *d*-*d* or charge-transfer type. Past attempts at definitive measurements claim NiO to be a charge-transfer insulator with a large insulating gap [ranging from 3.8 (Ref. 15) to 4.2 eV (Ref. 17)]. However, most measurement techniques are subject to dipole restrictions which do not allow direct measurements of the *d*-*d* gap arising from the Hubbard-split Ni 3*d* band. Such measurements would consistently result in optical transitions between states of *p* and *d* character, or in this case, charge-transfer transitions between the Ni *d* and O *p* states near E_F.

From our data presented in Figs. 3 and 4 it is evident that the top of the valence band consists primarily of *d*-character electron states, as has also been shown in results from other photoemission experiments.[43,44] Spectra in Fig. 5 also show the bottom of the conduction band to be of mostly *d* character, which is displayed in previously measured bremsstrahlung isochromat spectroscopy (BIS) spectra.[39,45] Studies concerning the magnitude of the insulating gap also lend support to the notion of it being characterized as a *d*-*d* gap with measurements of the energy difference between the Hubbard-split *d* minority bands being smaller than that of the charge-transfer transition. Resonant x-ray emission spectroscopy measurements also performed on our NiO single-crystal sample,[29] similar to previously published measurements,[25] show features corresponding to an absorp-

tion and emission energy loss of approximately 2 eV, a magnitude similar to results for the *d-d* transition energy (~2 eV) from SPEELS measurements,[23] SHG measurements,[21] and optical absorption measurements.[46] The magnitude of the dipole-allowed, charge-transfer optical gap between states of primarily O *p* and Ni *d* character appears to be considerably larger (~6 eV) than the gap between primarily *d*-character states. A second energy-loss peak is observed in the RXES measurements with a loss (~5 eV) in the spectral region where charge-transfer excitations are expected.

In measurements such as ours, excitonic effects inherent in the core-level x-ray processes can heavily influence the measured gap between the emitting and absorbing states. The Coulomb interaction between an excited electron coupled with the core-hole created influences the electron's binding energy,[47] and the intermediate state configuration resulting from core-level absorption is not equivalent to the configuration required for an absolute measurement of the transition across the insulating gap, due to a remaining Ni 2*p* core hole in what should be a complete shell. For this reason we cannot claim our comparison of absorption and emission spectra to be a measure of the true magnitude of the valence or conduction band gap of NiO. Although our NEXAFS absorption measurements show similarities to measurements performed using BIS, the ability to place an electron in an unoccupied state without creating a hole makes BIS a valid measurement of the conduction band.[45]

Our DOS calculations and XES and XAS (NEXAFS) measurements suggest that the number of O *p* states near E_F is much smaller (approximately 10%) than the number of Ni *d* states, a difference also amplified in the XES and XAS measurements by the dipole selection rule, which filters out emission and absorption states of *p* character at the Ni $L_{2,3}$ edge and states of *d* and *s* character at the O *K* edge. Our valence band measurements show no support for the notion that there is a definite band of O states between Hubbard-*U*-split Ni *d* states and the Fermi energy,[39,43] implying the insulating gap to be characterized by *d-d* transfer. However, the presence of O *p* states at the top of the valence and bottom of the conduction band combined with the nearly complete valence band hybridization displayed in the SSXPS measurements suggest the possibility of charge-transfer excitations across the band gap. Therefore we cannot simply assume NiO to be an insulator of Mott-Hubbard type based on the majority of states being Ni 3*d* states, it also has the properties of a charge-transfer system, befitting the intermediate region of the Zaanen-Sawatzky-Allen (ZSA) model.[48]

CONCLUSIONS

We have measured valence and excited states of NiO using atom- and site-specific XES and XAS (NEXAFS), and atom-enhanced SSXPS. By comparing our measurements to DOS calculations using the GGA within the DFT, we show valence as well as excited states to be nearly completely hybridized between Ni and O sites in ionic NiO. From this information we feel that the hybridization greatly affects characterization of the insulating gap in NiO, and suggests a combination Mott-Hubbard and charge-transfer character, as described by the ZSA model. While not representative of a true band gap measurement, our results show an insulating gap magnitude similar to other techniques used to measure *d-d* excitations in Hubbard split systems, and a considerably larger optical gap magnitude of charge-transfer excitations between O *p* and Ni *d* states.

ACKNOWLEDGMENTS

One of us (T.M.S.) would like to thank J. Jiménez-Mier for his assistance, and G. A. Sawatzky for providing comments on an earlier draft of this work. This work was supported in part by NSF Grant No. DMR9801804, and DOE-EPSCOR cluster research Grant No. DOE-LEQSF-03. The Advanced Light Source is supported by the Office of Basic Energy Sciences, U.S. Department of Energy Contract No. DE-AC03-76SF00098. The National Synchrotron Light Source is supported by the U.S. Department of Energy.

*Electronic mail: tschule@tulane.edu

†Current address: San Diego State University-IVC, 720 Herber Ave, Calexico, CA 92231, USA.

‡Current address: Department of Physics, University of South Florida, Tampa, FL 33620, USA.

[1] P. A. Cox, *Transition Metal Oxides*, 1st ed. (Oxford University Press, New York, 1992).

[2] F. M. F. de Groot, J. Electron Spectrosc. Relat. Phenom. **67**, 529 (1994).

[3] Z.-X. Shen, C. K. Shih, O. Jepsen, W. E. Spicer, I. Lindau, and J. W. Allen, Phys. Rev. Lett. **64**, 2442 (1990).

[4] S. M. Butorin, J.-H. Guo, M. Magnuson, P. Kuiper, and J. Nordgren, Phys. Rev. B **54**, 4405 (1996).

[5] N. F. Mott, Proc. Phys. Soc., London, Sect. A **62**, 416 (1949).

[6] J. Hubbard, Proc. R. Soc. London, Ser. A **276**, 238 (1963).

[7] C. Kittel, *Introduction to Solid State Physics* (Wiley, New York, 1986).

[8] T. Eto, S. Endo, M. Imai, Y. Katayama, and T. Kikegawa, Phys. Rev. B **61**, 14 984 (2000).

[9] O. Tjernberg, S. Söderholm, G. Chiaia, R. Girard, U. O. Karlsson, H. Nylén, and I. Lindau, Phys. Rev. B **54**, 10 245 (1996).

[10] L. Alberts and E. W. Lee, Proc. Phys. Soc. London **78**, 728 (1961).

[11] N. B. Weber, H. Ohldag, H. Gomonaj, and F. U. Hillebrecht, Phys. Rev. Lett. **91**, 237205 (2003).

[12] R. Gomez-Abal, O. Ney, K. Satitkovitchai, and W. Hübner, Phys. Rev. Lett. **92**, 227402 (2004).

[13] O. Tjernberg, S. Söderholm, U. O. Karlsson, G. Chiaia, M. Qvarford, H. Nylén, and I. Lindau, Phys. Rev. B **53**, 10 372 (1996).

[14] M. D. Towler, N. L. Allan, N. M. Harrison, V. R. Saunders, W. C. Mackrodt, and E. Aprà, Phys. Rev. B **50**, 5041 (1994).

[15] R. J. Powell and W. E. Spicer, Phys. Rev. B **2**, 2182 (1970).

[16] S. Hüfner, Solid State Commun. **53**, 707 (1985).
[17] G. A. Sawatzky and J. W. Allen, Phys. Rev. Lett. **53**, 2339 (1984).
[18] John P. Perdew and Mel Levy, Phys. Rev. Lett. **51**, 1884 (1983).
[19] F. Aryasetiawan and O. Gunnarsson, Phys. Rev. Lett. **74**, 3221 (1995).
[20] G. P. Zhang, T. A. Callcott, G. T. Woods, L. Lin, Brian Sales, D. Mandrus, and J. He, Phys. Rev. Lett. **88**, 077401 (2002).
[21] S. I. Shablaev and R. V. Pisarev, Phys. Solid State **45**, 1742 (2003).
[22] M. Fiebig, D. Fröhlich, Th. Lottermoser, V. V. Pavlov, R. V. Pisarev, and H.-J Weber, Phys. Rev. Lett. **87**, 137202 (2001).
[23] B. Fromme, Ch. Koch, R. Deussen, and E. Kisker, Phys. Rev. Lett. **75**, 693 (1995).
[24] B. Fromme, *d-d Excitations in Transition-Metal Oxides: A Spin-Polarized Electron Energy-Loss Spectroscopy (SPEELS) Study* (Springer-Verlag, Berlin, 2001).
[25] Hirofumi Ishii, Yoichi Ishiwata, Ritsuko Eguchi, Yoshihisa Harada, Masamitsu Watanabe, Ashish Chainani, and Shik Shin, J. Phys. Soc. Jpn. **70**, 1813 (2001); M. Magnuson, S. M. Butorin, A. Agui, and J. Nordgren, J. Phys.: Condens. Matter **14**, 3669 (2002).
[26] J. C. Woicik, E. J. Nelson, D. Heskett, J. Warner, L. E. Berman, B. A. Karlin, I. A. Vartanyants, M. Z. Hasan, T. Kendelewicz, Z. X. Shen, and P. Pianetta, Phys. Rev. B **64**, 125115 (2001).
[27] J. C. Woicik, E. J. Nelson, T. Kendelewicz, P. Pianetta, Manish Jain, Leeor Kronik, and James R. Chelikowsky, Phys. Rev. B **63**, 041403(R) (2001).
[28] J. J. Jia, T. A. Calcott, J. Yurkas, A. W. Ellis, F. J. Himpsel, M. G. Samant, J. Stöhr, D. L. Ederer, J. A. Carlisle, E. A. Hudson, L. J. Terminello, D. K. Shuh, and R. C. C. Perera, Rev. Sci. Instrum. **66**, 1394 (1995).
[29] T. M. Schuler, D. L. Ederer, S. Itza-Ortiz, G. T. Woods, T. A. Callcott, and J. C. Woicik (unpublished).
[30] J. A. Bearden and A. F. Burr, Rev. Mod. Phys. **39**, 125 (1967).
[31] F. M. F. de Groot, M. Grioni, J. C. Fuggle, J. Ghijsen, G. A. Sawatzky, and H. Petersen, Phys. Rev. B **40**, 5715 (1989).
[32] J. A. Bearden, Rev. Mod. Phys. **39**, 78 (1967).
[33] P. Blaha, K. Schwarz, and J. Luitz, Computer code WIEN97 (Technical Universität Wien, Austria, 1999).
[34] J. P. Perdew, K. Burke, and M. Ernzerhof, Phys. Rev. Lett. **77**, 3865 (1996).
[35] V. Ozolins and M. Körling, Phys. Rev. B **48**, R18 304 (1993).
[36] V. I. Anisimov, J. Zaanen, and O. K. Andersen, Phys. Rev. B **44**, 943 (1991).
[37] O. Bengone, M. Alouani, P. Blöchl, and J. Hugel, Phys. Rev. B **62**, 16 392 (2000).
[38] J. J. Yeh and I. Lindau, At. Data Nucl. Data Tables **32**, 1 (1985).
[39] S. Hüfner and T. Riesterer, Phys. Rev. B **33**, 7267 (1986); S. Hüfner, P. Steiner, I. Sander, F. Reinert, and H. Schmitt, Z. Phys. B: Condens. Matter **86**, 207 (1992).
[40] G. van der Laan, J. Zaanen, G. A. Sawatzky, R. Karnatak, and J.-M. Esteva, Phys. Rev. B **33**, 4253 (1986).
[41] J. Jiménez-Mier (private communication).
[42] L. A. Grunes, Phys. Rev. B **27**, 2111 (1983).
[43] Z. X. Shen, R. S. List, D. S. Dessau, B. O. Wells, O. Jepsen, A. J. Arko, R. Barttlet, C. K. Shih, F. Parmigiani, J. C. Huang, and P. A. P. Lindberg, Phys. Rev. B **44**, 3604 (1991).
[44] D. E. Eastman and J. L. Freeouf, Phys. Rev. Lett. **34**, 395 (1975).
[45] F. J. Himpsel and Th. Fauster, Phys. Rev. Lett. **49**, 1583 (1982).
[46] R. Newman and R. M. Cherenko, Phys. Rev. **114**, 1507 (1959).
[47] David Adler and Julius Feinleib, Phys. Rev. B **2**, 3112 (1970).
[48] J. Zaanen, G. A. Sawatzky, and J. W. Allen, Phys. Rev. Lett. **55**, 418 (1985).